COMPONENT PART NOTICE

THIS PAPER IS A COMPONENT PART OF THE FOLLOWING COMPILATION REPORT:

(TITLE): The Effect of the Ionosphere on Radiowave Signals and Systems Performance

Based on Ionospheric Effects Symposium Held on 1-3 May 1990.

(SOURCE): Naval Research Lab., Washington, DC

To ORDER THE COMPLETE COMPILATION REPORT USE AD-A233 797 .

THE COMPONENT PART IS PROVIDED HERE TO ALLOW USERS ACCESS TO INDIVIDUALLY AUTHORED SECTIONS OF PROCEEDINGS, ANNALS, SYMPOSIA, ETC. HOWEVER, THE COMPONENT SHOULD BE CONSI ED WITHIN THE CONTEXT OF THE OVERALL COMPILATION REPORT AND NOT AS A STAND-ALONE TECHNICAL REPORT.

THE FOLLOWING COMPONENT PART NUMBERS COMPRISE THE COMPILATION REPORT:

AD#:   TITLE:

AD-P006 265 thru AD-P006 325

DTIC
ELECTE
SEP 0 5 1991
S D
D

Accesion For

NTIS CRA&I	☑
DTIC TAB	[ ]
Unannounced	☐
Justification	

By
Distribution /

Availability Codes

Dist	Avail and/or Special
A-1	
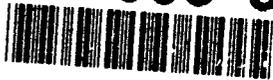
A GLOBAL IONOSPHERIC CONDUCTIVITY AND ELECTRON DENSITY (ICED) MODEL

Robert E. Daniell, Jr.
Computational Physics, Inc.
385 Elliot Street
Newton, MA 02072

Dwight T. Decker
Institute for Space Research
Boston College
Chestnut Hill, MA 02167

David N. Anderson and John R. Jasperse
Ionospheric Physics Division
Geophysics Laboratory
Hanscom AFB, MA 01731

Jan J. Sojka and R. W. Schunk
Center for Atmospheric and Space Sciences
Utah State University
Logan, UT 84322

ABSTRACT

At the Fifth Ionospheric Effects Symposium (IES '87), a paper was presented and published that described an operational Air Force Air Weather Service (AWS), near real-time, ionospheric specification model called Ionospheric Conductivity and Electron Density (ICED) . That version of the model specified primarily the northern hemisphere midlatitude and auroral zone ionospheric regions and did not cover either the low latitude or high latitude/polar cap regions. We are making extensions and modifications to ICED that provide a global specification — in effect a GLOBAL ICED. Major additions include (1) specification of electron and ion density profiles (90 to 1000 km) in the high latitude trough, auroral oval, and polar cap ionosphere in both northern and southern hemispheres, (2) midlatitude electron and ion density profiles that include magnetic declination effects, and (3) low latitude ionospheric specification that accounts for longitude control through differences in vertical $E \times B$ drift patterns. Since this model is driven by real-time data, we describe the various input parameters and how they are incorporated.

INTRODUCTION

The Ionospheric Conductivity and Electron Density (ICED) described by Tascione et al. [1988] provides near real-time specification of the northern midlatitude and auroral ionosphere ($20°N$ - $80°N$ corrected geomagnetic latitude) based on climatological models. The model is driven by two geophysical parameters: SSN_{eff}, an effective sunspot number (or ionospheric index) determined from the Air Weather Service real-time ionosonde network observations and Q_{eff}, an auroral activity index determined from satellite imagery. ICED was modified to include the low latitude ionosphere ($20°S$ - $20°N$) by including the Fully Analytic Ionospheric Model (FAIM) of Anderson et al. [1989], a parameterized version of the Semi-Empirical Low-latitude Ionospheric Model (SLIM) of Anderson et al. [1987] combined with a modified version of the Chiu [1975] model. However, this model is only accurate for the American longitudes where magnetic declination is relatively small.

ICED is now being modified to provide a truly global ionospheric specification ($90°S$ - $90°N$) driven by a variety of near real-time data including digital ionosonde data, total electron content data, in situ plasma density, temperature, and composition measurements, and satellite based ultraviolet airglow and auroral emission measurements. As part of this modification effort, ICED is being changed from a primarily climatological model to a more physically based model. GLOBAL ICED is divided into five regions: Northern High Latitude, Northern Midlatitude, Low Latitude, Southern

Midlatitude, and Southern High Latitude. The boundaries between these regions are dynamic in the sense that they are adjusted according to current conditions. For example, the boundary between the high latitude and midlatitude regions is the equatorward edge of the subauroral trough, which expands and contracts with magnetic activity. The northern high latitude region model is in the testing and validation phase, while the other regions are still in the development phase. The following sections describe the two high latitude models, the two midlatitude models, and the low latitude model.

In all regions, we have based the new models on parameterizations of physically based "first principles" ionospheric models rather than on statistical or climatological models. Although existing physical models are still inadequate for accurately specifying the state of the ionosphere based solely on a few solar and geophysical parameters and require too many computer resources to be used in real time, we believe that they provide more realistic representations of actual ionospheric structures than can be obtained from statistical models that, by their very nature, tend to wash out both temporal and spatial structure. In addition, the physical models give ion composition information unavailable from models based on ionosonde measurements alone. The challenge is to find representations of these physical models that can be driven by real time data using available computer resources.

PARAMETERIZING THE PHYSICAL MODELS

For this version of GLOBAL ICED we have chosen to parameterize the physical models in terms of geophysical environmental parameters by producing databases of ion density profiles on a latitude, longitude (or local time), and universal time grid for a range of environmental parameters. The precise choice of environmental parameters and their values depends on the ionospheric region. Seasonal variations are most important for the middle and high latitudes. Solar activity is an important parameter at all latitudes. Geomagnetic activity is mainly important at high latitudes, while the wind-driven E- and F-region dynamos are important for the formation of the equatorial anomaly. Since the physical models make intensive use of computer resources, we generally produce databases for high, moderate, and low values of each parameter.

Since each database for a given set of geophysical parameters must represent the ionosphere throughout the applicable region during a 24 hour period in universal time, they tend to be unwieldy. Therefore, the next step is the production of a semi-analytic representation based on discrete orthonormal functions. (Discrete orthogonal functions have their orthogonality properties defined by sums on discrete grids rather than by integrals over a continuous interval. The functions themselves may or may not be defined between the grid points.)

The first stage in the process is the approximation of altitude profiles of ion density using Empirical Orthonormal Functions (EOF's). The generation and use of EOF's is described in Secan and Tascione [1984] or Kutzbach [1967] and references therein. In short, the EOF's are the eigenvectors of the covariance matrices of the ion density profiles. If the database consists of N altitude profiles, $f(z_i)$, $(i=1,2,...M)$, the elements of the covariance matrix are

$$c_{ij} = \frac{1}{N} \sum_{n=1}^{N} f_n(z_i) f_n(z_j), \qquad i,j = 1,2,...M \qquad (1)$$

the high latitude databases, M = 37 and N = 5760 (20 latitudes, 24 local times, and 12 UT's).

The eigenvalues $(\lambda_m, m=1,2,...M)$ of a covariance matrix are real and non-negative, and the eigenvectors, $g_m(z_k)$, are automatically orthogonal and easily normalized. (See, e.g., Hildebrand [1965].) We order the eigenvalues so that $\lambda_m \geq \lambda_{m+1}$. An exact representation of the nth altitude profile, $f_n(z)$, is given by

$$f_n(z_m) = \sum_{k=1}^{M} a_{nk} g_k(z_m), \qquad m = 1,2,...M, \qquad 1 \leq n \leq N \qquad (2)$$

where

$$a_{nk} = \sum_{m=1}^{M} f_n(z_m) g_k(z_m) \qquad (3)$$

It can be shown that the RMS error due to truncating the series (2) at K terms is minimized when the g_k are the eigenvectors of the covariance matrix — rather than any other set of discretely

orthogonal functions (Secan and Tascione [1984] and references therein).

For the high latitude region, we have found it best to generate a separate set of EOF's for each database rather than one set for the entire group of databases. We have also found that the first six (out of 37) EOF's produce good approximations and that further improvement requires many more EOF's. Since the high latitude ionosphere has so much spatial and temporal structure, we expect that the other regions will require no more, and quite probably fewer, EOF's per database. Examples of EOF's for O^+, NO^+, and O_2^+ from one of the high latitude databases are shown in Figure 1.
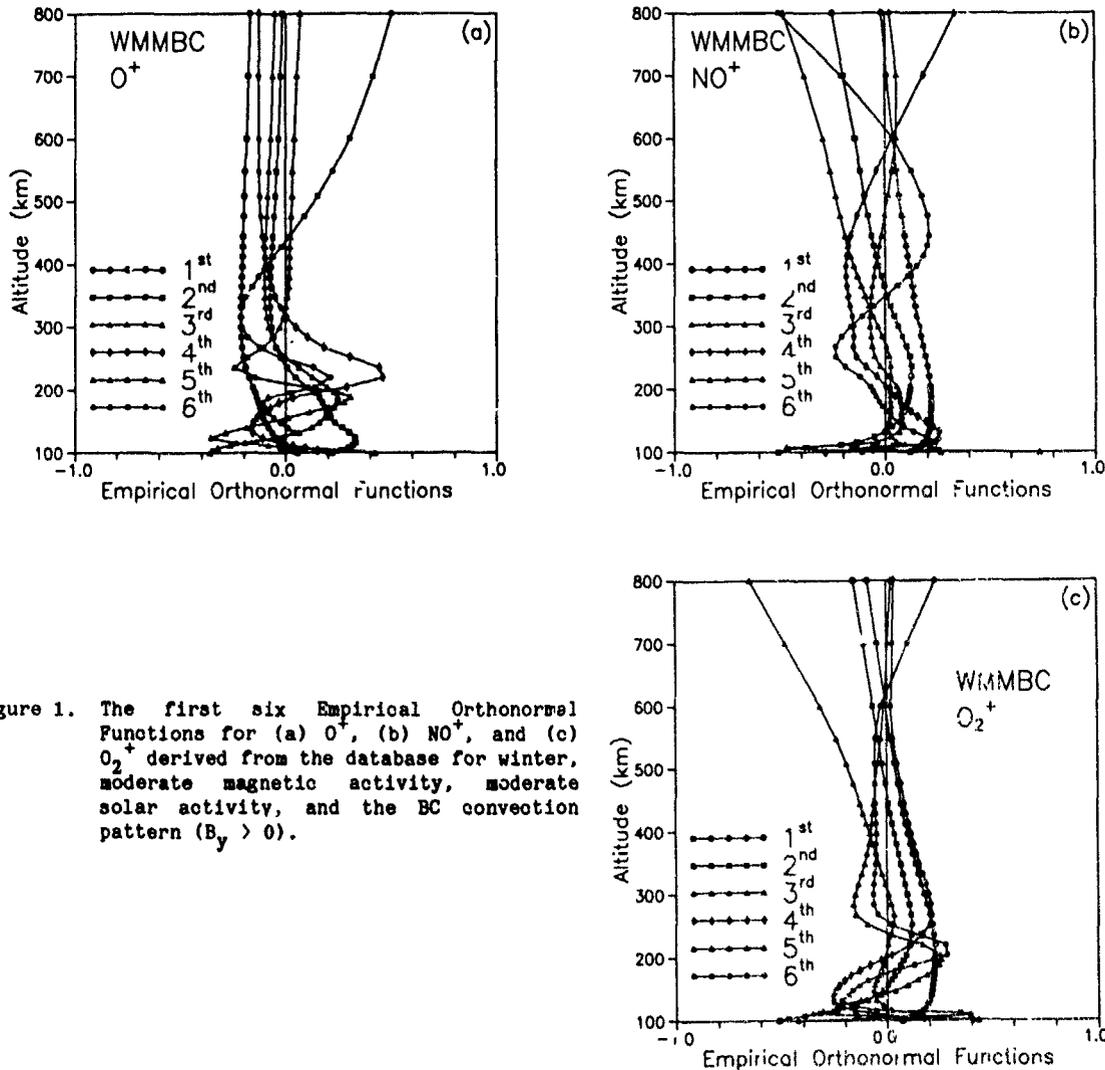
Figure 1. The first six Empirical Orthonormal Functions for (a) O^+, (b) NO^+, and (c) O_2^+ derived from the database for winter, moderate magnetic activity, moderate solar activity, and the BC convection pattern ($B_y > 0$).

The next stage involves the approximation of the horizontal variation of the EOF coefficients. If we were dealing with global databases, we would use some form of spherical harmonic expansion. However, since we are dealing with regions of limited latitude extent, there does not appear to be any special advantage to this approach, so we have chosen to attack each spatial variable in sequence.

For each universal time and magnetic latitude the coefficients, a_{nk}, of the EOF's are represented by Fourier series in magnetic local time (or longitude). (Trigonometric functions have the useful property that they are orthogonal n uniform discrete grids as well as on continuous intervals.) In the high latitude region, we used a nine term series (DC plus four cosine and four sine terms).

For each universal time the Fourier coefficients were represented by linear combinations of discrete orthonormal polynomials in magnetic latitude. These polynomials are generated for a given latitude grid by the algorithm of Beckman [1973]. We found that a nine term series gave a good representation of the latitude variations.

For the high latitude model, the low order polynomial coefficients showed primarily diurnal variations in universal time, but the higher order terms displayed considerably more structure. Consequently, we chose to tabulate the coefficients in UT and use polynomial interpolation rather than to use an orthogonal function expansion. This may not be necessary at middle and lower latitudes.

OPERATIONAL USE OF THE PARAMETERIZED MODELS

Once obtained, the semi-analytic representations of the physical models are used in two different ways. First, when real time ionospheric data are unavailable, they provide "best guesses" for the current state of the ionosphere based on estimates of the current levels of solar and geomagnetic activity. Second, when real time data are available, they are scaled to provide the best (least squares) fit to that data, and are used to give the altitude profile shapes. The way in which the parameterized model is scaled and adjusted by real time data depends on the region. One advantage of working with ion densities (rather than electron densities) is that the separation between the E-layer and F-layer can be made in a natural way: the molecular ions provide the E-layer while the atomic ions provide the F-layer.

The Northern and Southern High Latitude Regions

The high latitude ionosphere is very dynamic and highly structured making near real-time specification of electron density profiles extreme difficult. Fortunately, for many purposes it is the location of the structures that is of greatest interest with electron densities of lesser significance. We treat the E- and F-layers independently. For the F-layer, we divide the high latitude ionosphere into three sub-regions: the Trough, the Auroral Oval, and the Polar Cap.

The dynamic nature of the high latitude ionosphere is a direct result of the dynamic nature of the energy sources that drive it: magnetospheric convection and particle precipitation. Furthermore, the relatively long time scale of the F-layer (hours) implies that the current state of the ionosphere depends on recent history as well as current energy and momentum input. For this reason, even a perfect physical model would fail to accurately specify the current ionosphere unless it had accurate specifications of the recent history of the energy and momentum input. We have adopted a hybrid approach combining both empirical and physical models.

The physical model we adopted is the Utah State University high latitude ionospheric model [Schunk, 1988]. This model calculates ion and electron densities and temperatures by following flux tubes convecting through a moving neutral atmosphere. An analytic version [Rich and Maynard, 1989] of the convection model of Heppner and Maynard [1987] was used to specify the convection pattern for various levels of magnetic activity. Ionization rates due to particle precipitation were calculated using the Strickland et al. [1976] electron transport code and the electron precipitation model of Hardy et al. [1987]. Photoionization rates were calculated using photon fluxes from Hinteregger et al. [1977] and Heroux and Hinteregger [1978] (scaled with $F_{10.7}$) and the weighted cross sections of Torr et al. [1979].

The USU model was used to produce 54 databases containing NO^+, O_2^+, and O^+ densities as functions of altitude, magnetic latitude, magnetic local time, and universal time for a variety of environmental conditions. The specific parameters used were

    season: equinox: day 82 (March 23)
               June solstice: day 173 (June 22)
          December solstice: day 357 (December 23)

    solar activity ($F_{10.7}$): high (210), moderate (130), and low (70)

    magnetic activity (K_p): high (6.0), moderate (3.5), and low (1.0)

    Interplanetary magnetic field: B_z < 0 (southward)
                                      B_y > 0 (BC convection pattern)
                                      B_y < 0 (DE convection pattern)

Because of the uncertainty in convection patterns for B_z > 0 (northward), we made no calculations

354

for this case. Instead, we use the low magnetic activity cases to model B_z northward situations.

The first set of 54 databases were obtained for the northern hemisphere. Because the relationship between the magnetic and geographic poles is different in the two hemispheres, a second set of 54 databases is being generated for the southern hemispheres. This set will be treated in the same manner as the first set. The northern hemisphere databases have been approximated semi-analytically using EOF's, Fourier series, and discrete orthogonal polynomials as described in the previous section. Comparisons of the semi-analytic representations with the original databases are shown in Figure 2.

Figure 2. A comparison of ion density profiles from the original USU databases with the semi-analytic fits based on EOF's. These profiles are from the winter, high magnetic activity, high solar activity, B_y positive database. The fit is quite good except near the bottom where there is altitude structure not completely captured by the first six EOF's.
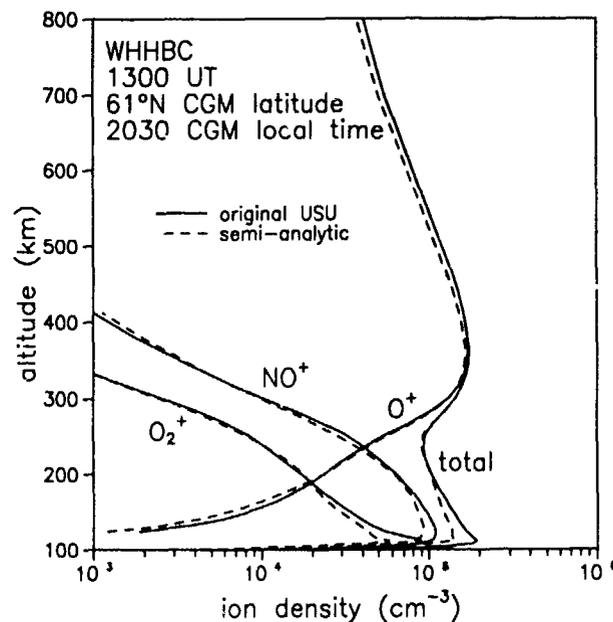
The real time specifications of the high latitude E- and F-layers are handled separately. This is appropriate because of the disparity in time scales associated with each altitude regime. The E-layer can be handled in two different ways. For post event analysis, when computer resources are abundant, a first principles chemical equilibrium model is used. Ion production rates can be determined from a combination of satellite based electron precipitation data, satellite borne nadir viewing UV and X-ray intensity data, and statistical models of precipitation patterns. For real time analysis, when computer resources are scarce, the semi-analytic representations of the molecular ion densities are scaled to provide a least squares fit to the relevant real time data (mainly ionosonde measurements of $f_o E$). In addition, if information on the location of the auroral oval is available (e.g., from precipitating particle measurements or from visible or UV imagery) the latitude scale is adjusted accordingly.

Unlike the mid- and low-latitude regions, the semi-analytic representation of the high latitude physical model is not directly scaled to fit the real-time F-layer data. Instead, simple semi-empirical models of the three F-layer subregions are used. These are models of $f_o F_2$ only, so the parameterized physical model is used to provide the shapes of the O^+ altitude profiles.

The F-layer trough. Our semi-empirical trough model is based on the studies of Whalen [1989]. There appear to be three different local time features that together make up the complete trough. In the afternoon sector from shortly after magnetic local noon and fading out between the terminator and magnetic local midnight is a stable feature closely related to the ionospheric convection pattern. Because of the long time scale associated with F-layer phenomena, this feature does not respond to the instantaneous convection pattern, but "averages" over conditions prevailing during the previous several hours. From the end of the afternoon trough until sunrise in the F-layer the observed trough appears to be the result of superimposing auroral density enhancements on top of the naturally decaying nighttime ionosphere. However, the equatorward edge of the auroral density enhancement does not necessarily coincide with the equatorward edge of the precipitation because of convection. Finally, a morning trough sometimes develops between local dawn and local noon. The

precise conditions under which this trough appears are not clear at this time.

In our model, the equatorward edge of the trough is continuous in local time and is described as a distorted circle with the same shape as the convection boundaries of Heppner and Maynard [1987]. The radius of the circle is treated as an adjustable parameter. The width and depth of each trough feature (afternoon, nighttime, and morning) are independently adjustable. In the absence of sufficient data to fix these parameters, the afternoon trough is assigned a nominal depth of 2.5 MHz and a nominal width of 5° latitude, while the nighttime and morning trough parameters are set to reproduce the midlatitude ionosphere. The O^+ densities calculated by the midlatitude models provide "boundary conditions," and the depth parameters are calculated relative to those densities.

The auroral F-layer. Because the auroral F-layer is controlled by several different and competing processes (e.g., precipitation and convection), and because it is of less interest than the auroral E-layer, we use a very simple model. The equatorward edge is simply the poleward edge of the trough, and the poleward edge is simply the equatorward edge of the polar cap. A single adjustable parameter describes the peak f_oF_2 relative to the f_oF_2 value at the polar cap boundary. Although the potential to adjust the location of the peak f_oF_2 is retained, under normal circumstances it is simply centered between the two boundaries.

The polar cap F-layer. The polar cap is the most difficult region to model, and in the absence of a dense network of high time resolution ionosondes, impossible to specify completely. Under B_z south conditions, convection brings high density daytime plasma into the polar cap. Because convection is rarely a steady process, the usual result is patches of varying size that move through the polar region. Under B_z north conditions, the polar cap ionosphere is more uniform, but density irregularities at various scales may still occur. We attempt only to provide a crude model of the background ionosphere and to give statistical information on the occurrence of patches. If possible, high time resolution digital ionogram data will be used to estimate the interpatch (background) f_oF_2 values, intrapatch f_oF_2 values, and the size and spacing of the patches. The background plasma density will be obtained by scaling the CCIR coefficients to digital ionosonde observations in the polar cap. In the absence of such measurements, the current effective sunspot number will be used.

We are currently in the process of testing and refining this part of the model. Two preliminary tests of the model using actual data are shown in Figures 3 and 4. In both cases, only ground based ionosonde data was used in the parameter adjustment process. Independent data was used to check the accuracy of the adjustment in reproducing ionospheric features.

Figure 3. A contour plot of f_oF_2 (MHz) in geographic coordinates based on ionosonde data taken at 1200 UT on 21 December 1981. Also shown are the locations of the afternoon and morning trough minima as determined from DE-2 in situ density measurements by Santimay Basu (personal communication). There were a total of five ionosonde stations reporting data in the high latitude region. The model required four iterations to converge to the configuration shown here.
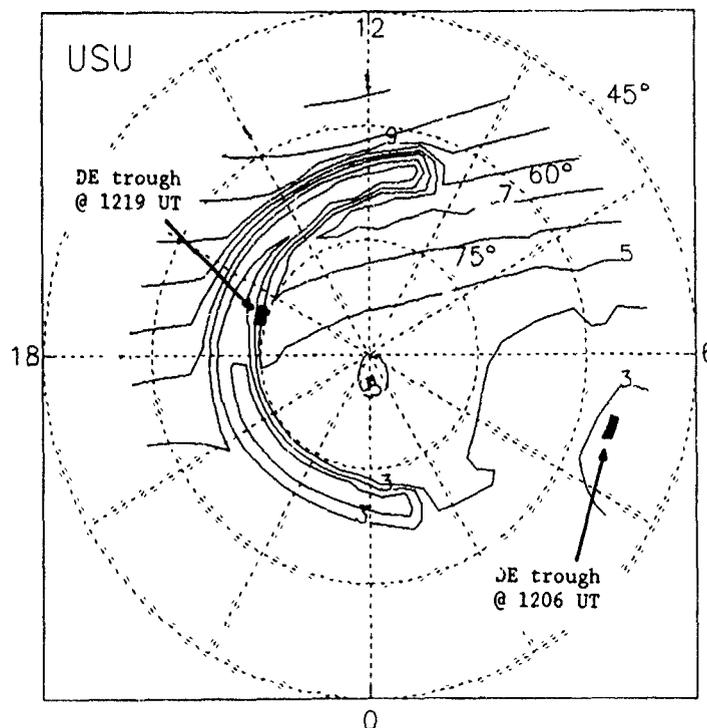
Figure 4. A contour plot of f_oE (MHz) at 0000 UT on 21 December 1981. Also shown is the equatorward boundary of the auroral oval (0.3 erg $cm^{-2} s^{-1}$) as determined from NOAA-6 data by H. W. Kroehl (personal communication). There were a total of seven ionosonde stations reporting high latitude information, of which only one reported E-layer data.

USU

45°

60°

75°

12

18

6

0

NOAA-6 auroral boundary @ 0003 UT
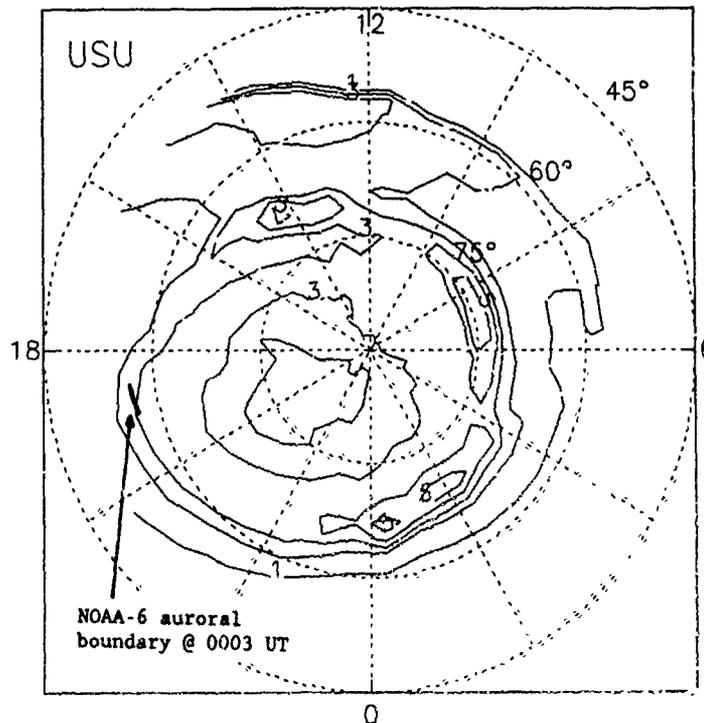
In both of these cases, reasonable agreement was obtained despite the limited data set used to drive the model. We anticipate even better accuracy in normal operation with a variety of near real time data available. After further testing and refinement, this model will be validated against an extensive set of data intended to resemble as closely as possible the expected complement of operational data.

The Northern and Southern Midlatitude Regions

The midlatitude ionosphere is less dynamic and less structured than the high latitude ionosphere. Consequently, it is not necessary to resort to semi-empirical subregion models. Furthermore, convection is unimportant so the IMF orientation may be ignored. Otherwise, the procedure is very similar to that used for high latitudes.

The midlatitude physical model is a combination of the photoelectron model of Jasperse [1981], a photochemical equilibrium E-layer model, and a midlatitude version of the F-layer (O^+) model of Anderson [1973].

The semi analytic representation of the midlatitude physical model is being produced by the same method used for the high latitude model. The real time operation will be somewhat different, however. A global ionospheric index, roughly corresponding to the SSN_{eff} of the original ICED, will be determined from the complete set of Air Weather Service digital ionosondes. This index will be used to scale the global model. However, regional indices will also be generated using ionosonde and other data (TEC, in situ plasma densities and temperatures, UV imagery, etc.). These indices will allow the ion density scalings to vary with spatial location, resulting in a more accurate representation of the ionosphere where data is abundant without introducing extraneous changes where data is absent. As with the high latitude data, the profile shapes come from the theoretical model, although the topside shapes will be modified where appropriate data is available. In particular in situ temperature, density, and composition measurements in the topside F-layer will be used to adjust the theoretical topside profiles to provide a more accurate representation.

357

The Low Latitude Region

The low latitude ionosphere has many of the characteristics of the high latitude ionosphere: it is dynamic and exhibits spatial structure. As for the polar cap, we do not attempt to specify the details of the small scale structure (bubbles, plumes, etc.). The incorporation of FAIM into ICED provided limited low latitude capability, primarily in the region of low magnetic declination. FAIM includes an analytic representation of the low latitude O^+ model of Anderson [1973, 1981] using ion drift data from Jicamarca [Woodman, 1970; Fejer et al., 1979] and assuming no magnetic declination effects. No additional real-time information (beyond SSN_{eff} and Q_{eff}) was incorporated in the model. We are using the same model (combined with our midlatitude E-layer model) along with additional data and a more realistic magnetic field as the basis for the GLOBAL ICED low latitude model. As in the high and middle latitude regions, the ability to adjust itself on the basis of near real time data will be an integral part of the model.

The semi-analytic representation of the physical model is obtained using the same methods as for the high and middle latitude regions. A series of databases is being produced for a range of environmental conditions. The altitude profiles will be represented by a linear combination of EOF's, and the coefficients will be represented by Fourier series in local time and discretely orthogonal polynomials in latitude.

The real time operation will make use of in situ electron density measurements and UV airglow images to determine the location of the equatorial anomaly peaks (or the width of the equatorial bulge when the anomaly is absent) to set the scale of the electric field. TEC data and/or UV and visible airglow measurements will be used to set the scale of the density. As in midlatitudes, adjustments will be made regionally as well as globally to produce the best least squares fit to the available data.

THE INTEGRATED MODEL: GLOBAL ICED

The five regional models are to be combined to produce a single GLOBAL ICED. The midlatitude model will be used to define the values of f_oF_2 at the equatorward edge of the trough, and these are fixed as "boundary conditions" on the high latitude F-layer model. Continuity of the O^+ profiles is insured by taking a weighted average of the mid-latitude and high-latitude profiles in the trough wall. Continuity of the E-layer (molecular ions) is insured by doing a similar weighted average over the same latitude range.

The boundary between the low and middle latitude regions is less sharply defined. Because the midlatitude and low latitude models are basically the same, the principle difference being the absence of electric fields in the midlatitude model, the two models must give the same results far enough from the magnetic equator. The latitude at which the two models agree will become the boundary between the two regions and will move according to actual conditions as detected in the real time data. Any minor discrepancy between the two models will be smoothed out by using a weighted average in the region of overlap.

Integration will proceed as soon as all the regional models have been tested, refined, and validated against actual data. Once integration is complete, GLOBAL ICED will undergo a final process of testing, refinement, and validation before being turned over to the Air Weather Service for conversion to operational use. We expect GLOBAL ICED to be complete by the end of 1991.

FUTURE DEVELOPMENT

We see GLOBAL ICED as the first step in the continued evolution of ICED. As scientific understanding of the physical processes that control the ionosphere continues to improve, and as computers continue to become more powerful, we expect the physical basis of the model to become stronger and the reliance on semi-empirical models and semi-analytical parameterizations to be reduced. The ultimate goal is a unified first principles model running in real time with periodic adjustments from real time measurements to compensate for the uncertainties inherent in any attempt to specify the global energy and momentum inputs to the ionospheric system. We also have begun the process of developing a limited forecast model whose evolution will parallel that of ICED.

REFERENCES

Anderson, D. N., A theoretical study of the ionospheric F region equatorial anomaly, 1, Theory, Planet. Space Sci., 21, 409-419, 1973.

Anderson, D. N., M. Mendillo, and B. Hernater, A Semiempirical Low-latitude Ionospheric Model, Radio Sci., 22, 292-306, 1987.

Anderson, D. N., J. M. Forbes, and M. Codrescu, A Fully Analytic, Low- and Middle-Latitude Ionospheric Model, J. Geophys. Res., 94, 1520-1524, 1989.

Chiu, Y. T., An Improved Phenomenological Model of Ionospheric Density, J. Atmos. Terr. Phys., 37, 1563-1570, 1975.

Fejer, B. G., D. T. Farley, R. F. Woodman, and C. Calderon, Dependence of equatorial F region vertical drifts on season and solar cycle, J. Geophys. Res., 84, 5792-5796, 1979.

Hardy, D. A., M. S. Gussenhoven, R. Raistick, and W. J. McNeil, Statistical and Functional Representation of the Pattern of Auroral Energy Flux, Number Flux, and Conductivity, J. Geophys. Res., 92, 12275-12294, 1987.

Heppner, J. P., and N. C. Maynard, Empirical High-Latitude Electric Field Models, J. Geophys. Res., 92, 4467-4489, 1987.

Heroux, L., and H. E. Hinteregger, Aeronomical reference spectrum for solar UV below 2000 Å, J. Geophys. Res., 83, 5305-5308, 1978.

Hildebrand, F. B., Methods of Applied Mathematics, Prentice-Hall, Englewood Cliffs, pp. 30-34, 1965.

Hinteregger, H. E., D. E. Bedo, J. E. Manson, and D. R. Skillman, EUV flux variations with solar rotation observed during 1974-1976 from the AE-C satellite, Space Res., 17, 533-544, 1977.

Jasperse, J. R., The photoelectron distribution function in the terrestrial ionosphere, in Physics of Space Plasmas, ed. by T. S. Chang, B. Coppi, and J. R. Jasperse, Scientific Publishers, Cambridge, MA, pp. 53-84, 1982.

Kutzbach, J. E., Empirical Eigenvectors of Sea-Level Pressure, Surface Temperature, and Precipitation Complexes over North America, J. Appl. Meteor., 6, 791, 1967.

Rich, F. J., and N. C. Maynard, Consequences of Using Simple Analytical Functions for the High-Latitude Convection Electric Field, J. Geophys. Res., 94, 3687-3701, 1989.

Schunk, R. W., A Mathematical Model of the Middle and High Latitude Ionosphere, Pageoph, 127, 255-303, 1988.

Secan, J. A., and T. F. Tascione, The 4D Ionospheric Objective Analysis Model, in Proceedings of the 1984 Ionospheric Effects Symposium, ed. by Goodman, Klobuchar, and Soicher, 336-345, 1984.

Strickland, D. J., D. L. Book, T. P. Coffey, and J. A. Fedder, Transport Equation Techniques for the Deposition of Auroral Electrons, J. Geophys. Res., 81, 2755-2764, 1976.

Tascione, T. F., H. W. Kroehl, R. Creiger, J. W. Freeman, R. A. Wolf, R. W. Spiro, R. V. Hilmer, J. W. Shade, and B. A. Hausman, New Ionospheric and Magnetospheric Specification Models, Radio Sci., 23, 211-222, 1988.

Torr, M. R., D. G. Torr, R. A. Ong, and H. E. Hinteregger, Ionization frequencies for major thermospheric constituents as a function of solar cycle 21, Geophys. Res. Lett., 10, 771-774, 1979.

Whalen, J. A., The Daytime F Layer Trough and Its Relation to Ionospheric-Magnetospheric Convection, J. Geophys. Res., 94, 17169-17184, 1989.

Woodman, R. F., Vertical drift velocities and east-west electric fields at the magnetic equator, J. Geophys. Res., 75, 6249-6259, 1970.